JMEPEG (2013) 22:3155–3160
DOI: 10.1007/s11665-013-0601-4

1059-9495/$19.00

Evaluation of Hard Coating Performance in Drilling Compacted Graphite Iron (CGI)

José M.F.de Paiva Jr., Fred L. Amorim, P. Soares, and Ricardo D. Torres

(Submitted August 31, 2012; in revised form April 23, 2013; published online May 30, 2013)

The aim of this investigation was to compare the performance of the following commercial coatings system, TiAlN/TiN, AlCrN, and TiSiN/AlCrN, deposited in cemented carbide tools in drilling compact graphite iron (CGI). The drilling tests were conducted adopting two cutting speeds: 80 or 150 m/min. For each test condition, the tool flank wear, the machining feed force, and the circularity and the roughness of the resulting drilled hole were determined. At the cutting speed of 80 m/min, the results revealed that the tool life, in terms of flank wear, was improved for the Cr-based coatings, while the multilayered coatings presented a better performance at the cutting speed of 150 m/min. It was also found that feed force is substantially increased when drilling at a cutting speed of 150 m/min. The holes drilled with the TiSiN/AlCrN at a cutting speed of 150 m/min showed the best circularity. The drill roughness is directly influenced by the coating system wear and iron adhesion. Consequently, it was found that the lowest holes' roughness was obtained with TiSiN/AlCrN at 80 m/min.

Keywords compacted graphite iron, hard coatings, machining, wear of cutting tools

1. Introduction

In relation to the traditional machining processes, drilling is one of the most important metal-cutting techniques; this process comprises approximately 33% of all metal-cutting operations (Ref 1). The drilling technology is being developed and implemented in response to new demands in terms of productivity, flexibility, accuracy, and environmental requirements. For instance, one of the last upcoming designs by the car markers is the fabrication of small diesel engines with compact graphite iron (CGI) instead of the traditional gray casting iron (CI). The compact graphite iron, due to its graphite morphology, presents higher strength which allows the fabrication of smaller engines with higher efficiency than the traditional gray casting iron engines. The major disadvantage of CGI is its poor machinability compared to CI. The formation of MnS layer during machining of CI allows the use of high cutting speeds, decreasing the engine production costs. The MnS layer cannot be formed in CGI due to the higher magnesium content necessary to form the compact graphite shape. The absence of MnS inclusion along with the interconnected morphology of the graphite reduces the tool life by about a factor of 20 when machining CGI (Ref 2-6).

There are two major cutting technologies to machine CGI. The first alternative is to machine CGI applying ceramic tools such as boron nitride inserts (Ref 6). The main disadvantage of applying ceramic inserts is the cost. The second and more common adopted solution in machining CGI is the use cemented carbide tools coated with hard PVD coatings. It well known that a deposition of hard coatings increases the tool life due to the increase in the tool surface hardness and isolation of the tool cutting edge from the extremely severe machining environment, such as high pressure and high temperature. In addition, the coating must provide higher abrasive wear and oxidation resistance, once the CGI microstructure is nearly fully perlitic, which generates high temperatures in the tool cutting edge (Ref 7-9).

The mechanical properties of PVD hard coatings such as AlCrN and TiSiN/AlCrN deposited over cemented carbide were investigated by Bourhis et al. (Ref 10). They found that AlCrN has an elastic modulus (E) of 394 GPa and hardness (H) of 30 ± 5 GPa, while TiSiN/AlCrN has an E of 315 GPa and H of 31 ± 5 GPa. The TiAlN/TiN multilayer coatings have been extensively characterized in terms of mechanical and microstructural properties. In the work by Weber et al. (Ref 11), they show that the compressive stress in the multilayer TiAlN/TiN changes with the deposition bias voltage. The highest compressive stress is observed for TiAlN/TiN, in which the Al/Ti ratio is 1.8, when the deposition bias voltage was −100 V. The reported hardness for the TiAlN/TiN system is around 35 GPa (Ref 12).

Abrasion tests were conducted in TiAlN and AlCrN coating by Kalss et al. (Ref 13); they conclude that the Cr-based coating presented a better abrasive resistance than TiAlN coatings. It has also been reported, by the same author, that thermal conductivity of AlCrN decreases above 250 °C, while the thermal conductivity of TiAlN increases with temperature and it is higher than the thermal conductivity of AlCrN. Moreover, the thermal stability of the Cr-based coating can be as high as 1100 °C, while the thermal stability of TiAl-based coatings and TiN is 800 and 600 °C, respectively (Ref 14).

In the present work, the effect of Cr content and coating system architecture was tested in drilling compacted graphite

José M.F.de Paiva Jr., Technological Innovation Center, Faculdade de Tecnologia Senai, Joinville, Brazil; and **Fred L. Amorim, P. Soares,** and **Ricardo D. Torres**, Mechanical Engineering Department, Pontificia Universidade Católica do Paraná, Curitiba, Brazil. Contact e-mail: ricardo.torres@pucpr.br.

iron. There is a lack of knowledge about the coatings' performance in drilling this new ferrous system. The coating systems investigated in this work were the following commercial coatings: TiAlN/TiN, AlCrN, and TiSiN/AlCrN. In this project, the cutting speed was varied and its effect on the coated tool flank wear was evaluated. Then, the effect of the drill flank wear in the feed force and the quality of the resulting drilled holes were determined.

2. Experimental Procedure

2.1 Coating System Characteristics and Workpiece Material

In this work, K10 cemented carbide straight flute drills were coated with three commercial coatings: TiAlN/TiN (Ref 11, 12), AlCrN, or TiSiN/AlCrN (Ref 9); the last two coatings were produced according to the Oerlikon Balzers Balinit Alcrona and Balinit Helica process, respectively. The coatings' thicknesses were between 2 and 3 μm. The drill's roughness after deposition of the coating systems was around 0.05 Ra.

The workpiece material was compacted graphite iron, class CGI 450. The CGI chemical composition, in wt.%, was C = 3.62%, Si = 2.41%, Mn = 037%, Cu = 1.17%, Sn = 0.064%, and Cr = 0.029%. The optical microscopy inspection of the CGI 450 revealed that the microstructure was nearly fully perlitic with hardness around 254 HB. Two sets of CGI specimens were cast in the form of slabs and disks. The two CGI specimens' geometries are shown in Fig. 1. The slab specimens were used for the flank wear evaluation tests, while the disk specimens were used for cutting forces measurement. The cutting parameters used in this investigation were a cutting speed of 80 or 150 m/min and a feed rate of 0.1 mm/rot.

2.2 Flank Wear Measurements

The straight flute drill flank wear was assessed using a Carl Zeiss Jena optical microscope, in which the magnification and resolution were 60× and 0.01 mm, respectively. In the flank wear evaluation, blind holes of 20 mm depth were drilled in the CGI slabs; this depth was achieved in two steps of 10 mm each. The flank wear measurements were done at every cutting length of 0.64 m, which corresponds to 32 drilled holes. At this cutting interval, the drill was taken off the CNC machine Center (Cincinnati Arrow 500, USA), placed in a clapping device that was under the optical microscope, and then the drill flank wear was determined. After the flank wear determination, the tool was returned to the CNC machine to continue the drilling process. The sequence of the flank wear determination is shown in Fig. 2. The flank wear tests were conducted under lubrication using LANOCENT 25 fluid produced by Solgren of Brazil.

2.3 Coated Tool Surface Characterization

After the drilling process, all three coated tool surfaces were examined under Jeol 6360-LV SEM. In the SEM facility, BSE imaging and EDS Characterization were performed.

2.4 Cutting Force Tests

The Cutting tests were carried out in a CNC machine Center (Cincinnati Arrow 500, USA). To evaluate the cutting forces, the CNC machine center was equipped with a Dynamometer (KYSTLER 9257 B, Switzerland) mounted under the CGI disk specimens. The cutting forces were measured in the coated tools at the following flank wear: 0, 0.2, and 0.4 mm. At this specific tool flank wear, holes of 20 mm were drilled in the CGI disks while the cutting forces were monitored. The cutting force measurements were done using the same cutting fluid used in the flank wear tests. Even though all the cutting force components were determined, the feed force was chosen to represent the effect of the tool flank wear in machining cutting forces.

2.5 Roundness Tests

The holes' circularity measurements were done using a Talyrond 232—Taylor Hobson equipment—using a 0.8 mm spherical probe. The roundness was taken in three positions in the drilled holes as follows: 5, 10, and 15 mm measured from the top of drilled hole.

2.6 Roughness Tests

The Ra roughness measurements were done using a Form TalySurf 50Ai—Taylor Hobson equipment—using a 2-mm spherical probe. The cutoff length was 0.8 mm and the total probed length was 4 mm. The Ra roughness was taken in depths between 10 and 15 mm from the top of the drilled hole.

3. Results and Discussion

3.1 Wear of the Coated Tool Cutting Edge

Figure 3 shows the SEM-BSE images of the tools' cutting edge after the drilling process. In these images, it is possible to differentiate the white and gray areas in the tools' cutting edge. The gray areas are an iron-based adherent material as revealed by the EDS spectrum in Fig. 4. On the other hand, the white areas, in the tools' cutting edge, are tungsten that comes from the tool substrate, which is tungsten cemented carbide. Interestingly, the EDS spectra in Fig. 4 do not show peaks of the coating system elements such as Ti, Cr, Si, and Al. For the AlCrN and TiSiN/AlCrN, the area of iron adhesion is higher for the tools in which the cutting speed was 150 m/min. For TiAlN/TiN, the aspect of the adhesion is practically the same for both cutting speeds. From this result, we can say that the tools' surface damage is taking place in two steps. In the first step, the coating system is removed from the tool surface. In the second step, there is an adhesion of iron in the unprotected tool cutting edge.

The flank wear as a function of the machined length shown in Fig. 5 agrees with the above observations. At a cutting speed of 80 m/min for AlCrN and TiSiN/AlCrN coating systems, one can observe a three-stage flank wear curve. In the first part of this curve, the flank wear rate is high due to the fact that a very high load is applied in a small area of the cutting edge; in this part of the wear behavior, the asperities plastically deform (Ref 15). In the second part of the wear curve, the contact area between the drill and the CGI counterpart becomes larger. Consequently, plastic flow no longer takes place and the coating system is continuously removed probably by abrasion since the CGI presents a fully perlitic microstructure where iron carbide is approximately 11 wt.%. In the third part of the wear curve, the coating is completely removed from the tool cutting

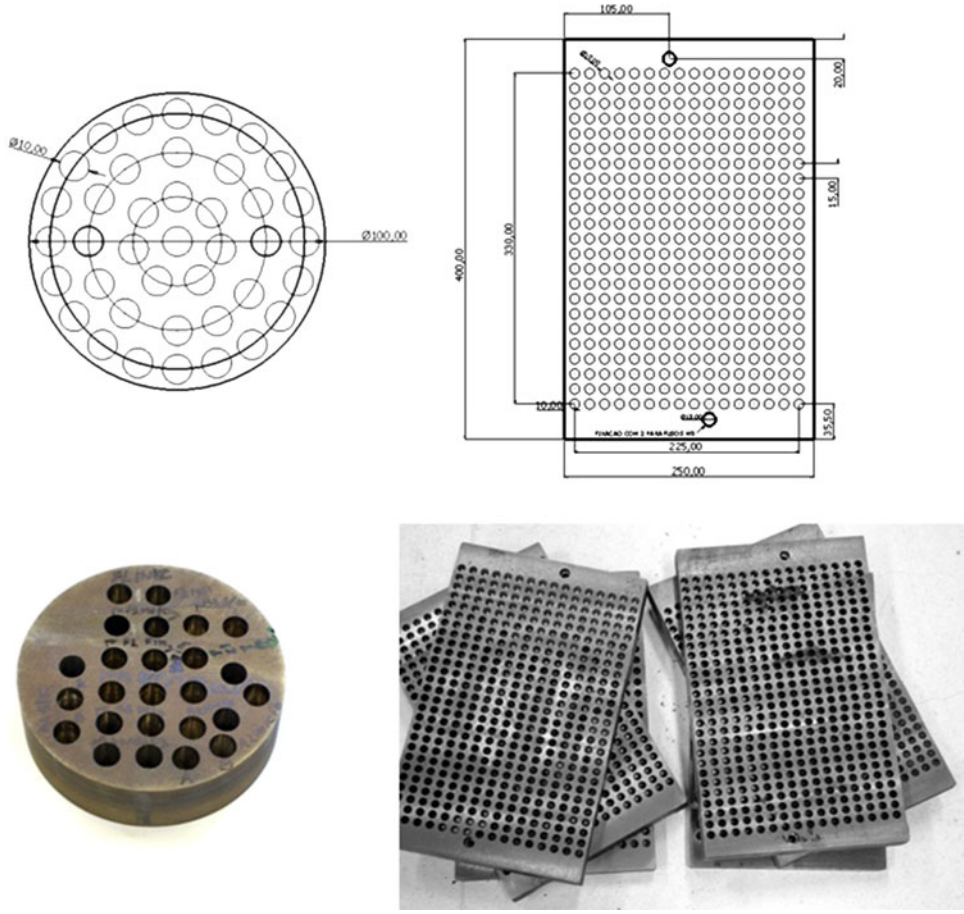

Fig. 1 Compacted graphite iron specimens' dimensions (in mm)

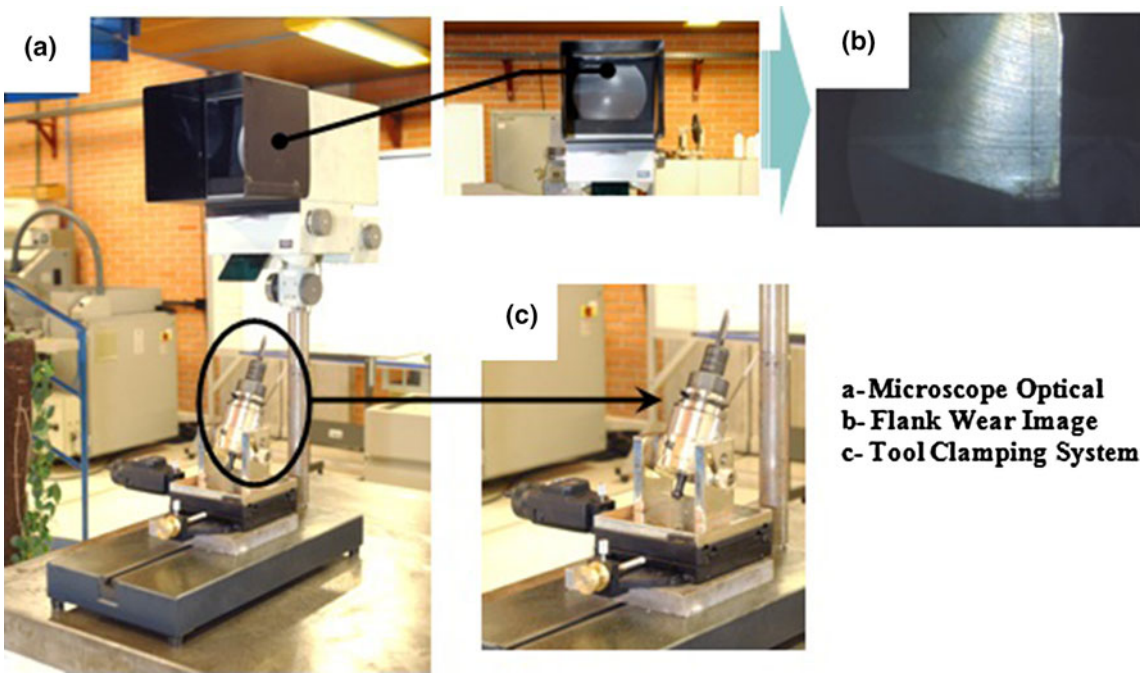

Fig. 2 Flank wear measurement devices

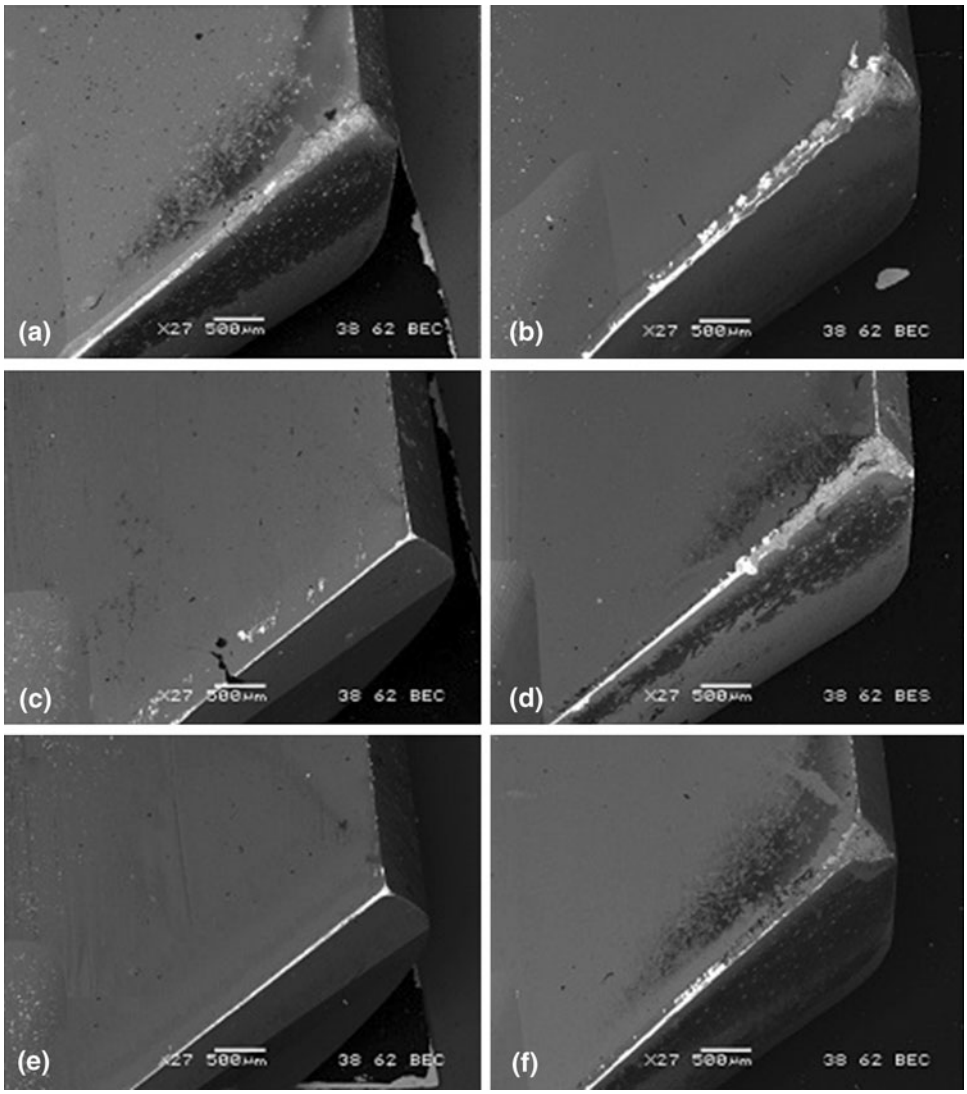

Fig. 3 SEM-BSE images showing the aspect of tools' cutting edges after drilling CGI. TiAlN/TiN at (a) 80 m/min and (b) 150 m/min; AlCrN at (c) 80 m/min and (d) 150 m/min; and TiSiN/AlCrN at (e) 80 m/min and (f) 150 m/min

edge and the tool substrate was exposed to high temperatures caused by the cutting process, leading to very rapid surface degradation. The iron adhesion starts to take place as soon as the substrate is exposed, being more intensive in the third part of wear curve. For the TiAlN/TiN, wear rate is high, even at 80 m/min, due to its lower thermal stability that favors particle removal probably by oxidation and abrasion, while the presence of Cr and Al, in the case of the AlCrN coating, and Si, Al, Cr, in the case of TiSiN/AlCrN, gives these two coating systems an improved thermal stability as was discussed earlier (Ref 14). At the cutting speed of 150 m/min, the three coating systems showed a very high flank wear rate in comparison with the coating performance observed at 80 m/min. Even though the three coating systems showed a similar behavior at this cutting speed, it is possible to observe a slightly improved performance of the multilayer coatings TiAlN/TiN and TiSiN/AlCrN.

3.2 Feed Force Versus Flank Wear

Figure 6 presents the feed force as function of the flank wear. In the feed force/flank wear curves, one can realize that the magnitude of the feed force is determined by the cutting speed. At 80 m/min, the TiAlN/TiN presented a higher feed force than the Cr-based coatings; at this cutting speed, the TiAlN/TiN presented a larger iron adhesion as can be visualized in Fig. 3. On the other hand, AlCrN and TiSiN/AlCrN showed a smaller feed force magnitude which is related to the smaller degradation of the tool surface when compared to the TiAlN/TiN coating system. For the cutting speed of 150 m/min, the feed force increases with the flank wear for all three coating systems.

3.3 Quality of Drilled Hole

The quality of the drilled holes was evaluated by performing roundness error and roughness tests. In Fig. 7 is presented the circularity of the drilled holes as function of the tool flank wear for the three coating systems. From this result, one can realize that the circularity is improved when drilling at 150 m/min. Figure 7 also shows that in the beginning of the drilling process the circularity is the lowest; as the cutting process progresses, the roundness error increases in a different fashion, depending on cutting speed and coating system. The coating system that

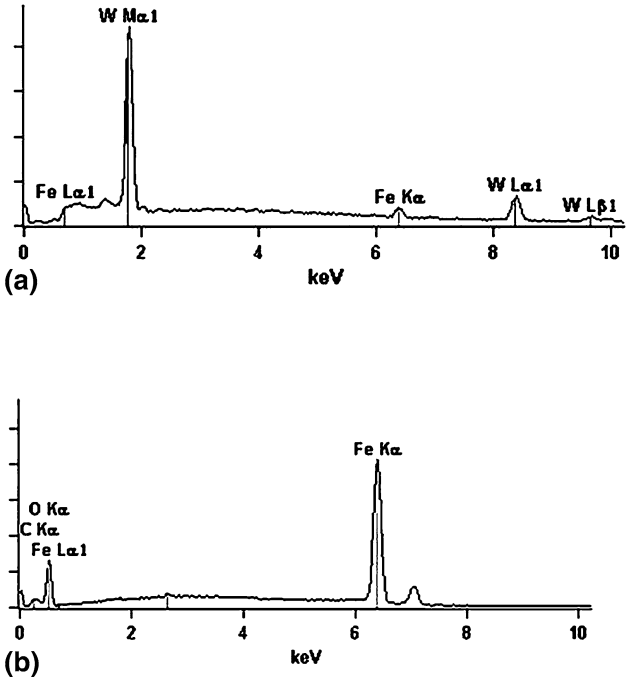

Fig. 4 SEM image and EDS spectra of the cutting edge after drilling CGI. (a) White areas and (b) gray areas in Fig. 3

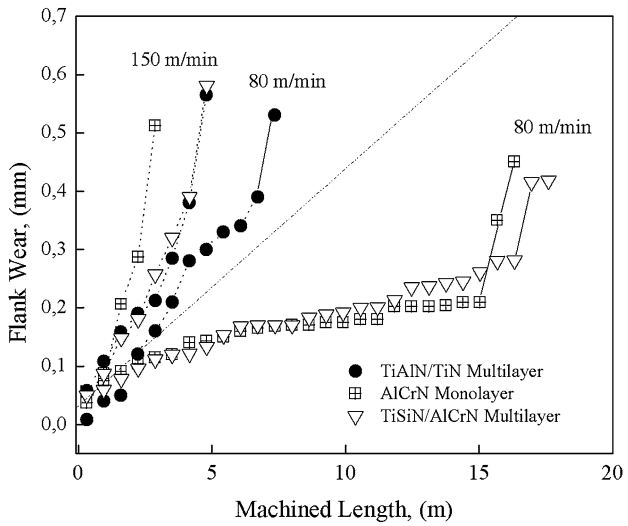

Fig. 5 Tool flank wear vs. machined length

produced the lowest role circularity variation with flank wear was the TiSiN/AlCrN system followed by the TiAlN/TiN system. The question to be addressed is why the circularity of the holes is better when machining at 150 m/min, if this cutting speed produces a large area of iron stick material. The answer to this issue is related to the tool cutting edge and CGI counterpart contact time, which is shorter when drilling at 150 m/min; shorter cutting times lessen the effect of degraded tool cutting edge in the roundness of the drilled hole. On the other hand, the roughness of the drilled hole is lower when drilling at 80 m/min as shown in Fig. 8. At the beginning of the drilling process, the multilayer coating produced a smoother drilled surface than the monolayer AlCrN. With the progress of the drilling process, the Cr-based coating produced a lower

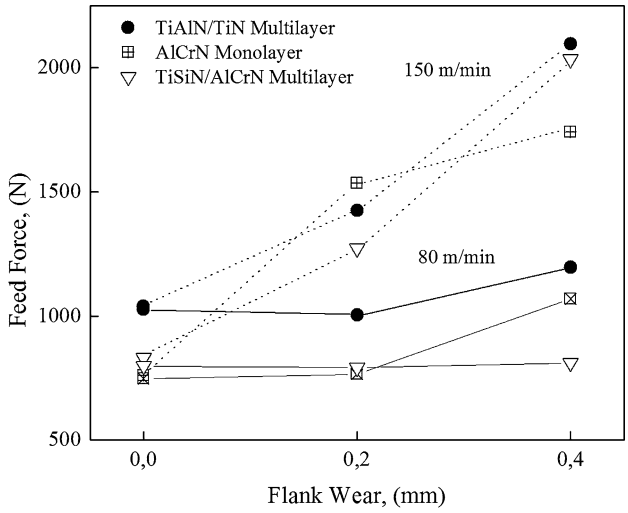

Fig. 6 Feed force vs. flank wear

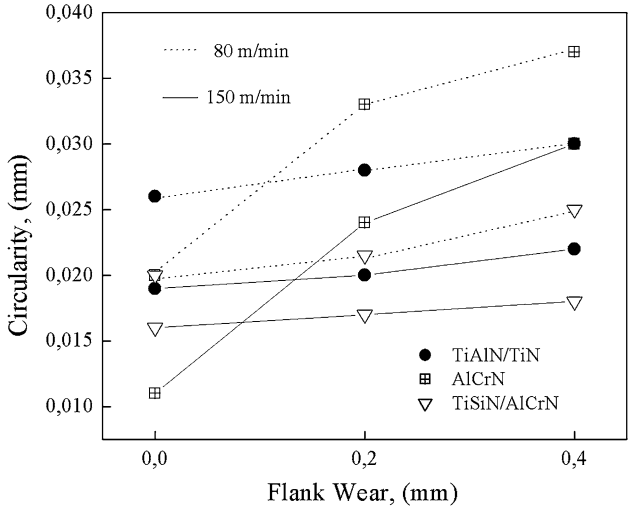

Fig. 7 Circularity of the drilled holes vs. flank wear

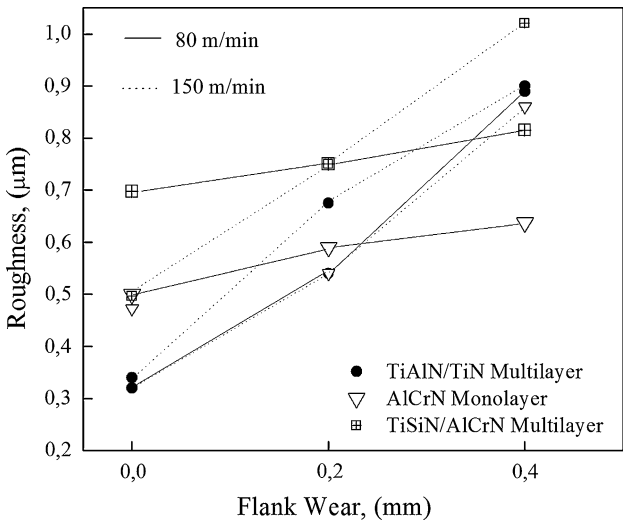

Fig. 8 Roughness of the drilled holes vs. flank wear

change in the roughness of the drilled holes. This observation is related to the wear fashion of the three coatings. In addition, examining the aspect of the tools' cutting edges in Fig. 3, one can realize that the amount of worn area and iron adhesion is the highest for the TiAlN/TiN coating system producing the highest roughness of the drilled holes even at 80 m/min. The roughness of the machined surface is directly influenced by the surface integrity of the tool used to machine it.

4. Conclusions

At a cutting speed of 80 m/min, the wear mechanism led to very slow wear and adhesion for the Cr-based coating, while for the TiAlN/TiN there was a fast wear of the tool cutting edge. At a cutting speed of 150 m/min, wear and iron adhesion become more intense. Consequently, all three coating systems failed very rapidly. Increasing the cutting speed from 80 to 150 m/min resulted in an increase in the feed force as result of the wear and adhesion, which is more severe at a higher cutting speed. The quality of the drilled hole evaluated through circularity and roughness revealed two trends. The circularity quality is directly related to the cutting speed. At a given coating system, the higher the cutting speed, the better the circularity. While the roughness is directly influenced by the coating system wear and adhesion, using lower cutting speed reduces the amount of wear and iron adhesion in the tool cutting edge, resulting in a lower surface roughness.

References

1. H.K. Toenshoff, W. Spintig, W. Koenig, and A. Neisses, Machining of Holes Developments in Drilling Technology, *Ann. CIRP*, 1994, **43**(2), p 551
2. M.B. da Silva, V.T.G. Naves, J.D.B. Melo, C.L.F. de Andrade, and W.L. Guesser, Analysis of Wear of Cemented Carbide Cutting Tools During Milling Operation of Gray Iron and Compacted Graphite Iron, *Wear*, 2011, **271**, p 2426–2432
3. M. Heck, H.M. Ortner, S. Flege, U. Reuter, and W. Ensinger, Analytical Investigations Concerning the Wear Behaviour of Cutting Tools Used for the Machining of Compacted Graphite Iron and Grey Cast Iron, *Int. J. Refract. Met. Hard. Mater.*, 2008, **26**, p 197–206
4. F. Mocellin, E. Melleras, W.L. Guesser, and L. Boehs, Study of the Machinability of Compacted Graphite Iron for Drilling Process, *J. Braz. Soc. Mech. Sci. Eng.*, 2003, **26**(1), p 22–27
5. E. Abele, A. Saham, and H. Schulz, Wear Mechanism When Machining Compacted Graphite Iron, *CIRP Ann. Manuf. Technol.*, 2002, **51**(1), p 53–56
6. M. Gastel, C. Konetschny, U. Reuter, C. Fasel, H. Schulz, R. Riedel, and H.M. Ortner, Investigation of the Wear Mechanism of Cubic Boron Nitride Tools Used for the Machining of Compacted Graphite Iron and Grey Cast Iron, *Int. J. Refract. Met. Hard. Mater.*, 2000, **18**, p 287–296
7. A.E. Reiter, V.H. Derflinger, B. Hanselmann, T. Bachmann, and B. Sartory, Investigation of the Properties of $Al_{1-x}CrxN$ Coatings Prepared by Cathodic Arc Evaporation, *Surf. Coat. Technol.*, 2005, **200**, p 2114–2122
8. J.L. Endrino, G.S. Fox-Rabinovich, A. Reiter, S.V. Veldhuis, R. Escobar Galindo, J.M. Albella, and J.F. Marco, Oxidation Tuning in AlCrN Coatings, *Surf. Coat. Technol.*, 2007, **201**, p 4505–4511
9. J.L. Mo, M.H. Zhu, B. Lei, Y.X. Leng, and N. Huang, Comparison of Tribological Behaviours of AlCrN and TiAlN Coatings—Deposited by Physical Vapor Deposition, *Wear*, 2007, **263**, p 1423–1429
10. E. Le Bourhis, P. Goudeau, M.H. Staia, E. Carrasquero, and E.S. Puchi-Cabrera, Mechanical Properties of Hard AlCrN-Based Coated Substrates, *Surf. Coat. Technol.*, 2009, **203**, p 2961–2968
11. F.-R. Weber, F. Fontaine, M. Scheib, and W. Bock, Cathodic arc Evaporation of (Ti, Al)N Coatings and (Ti, Al)N/TiN Multilayer-Coatings—Correlation Between Lifetime of Coated Cutting Tools, Structural and Mechanical Film Properties, *Surf. Coat. Technol.*, 2004, **177-178**, p 227–232
12. Shiva. Kalidas, Richard.E. DeVor, and Shiv.G. Kapoor, Experimental Investigation of the Effect of Drill Coatings on Hole Quality Under Dry and Wet Drilling Conditions, *Surf. Coat. Technol.*, 2001, **148**, p 117–128
13. W. Kalss, A. Reiter, V. Derflinger, C. Gey, and J.L. Endrino, Modern Coatings in High Performance Cutting Applications, *Int. J. Refract. Met. Hard. Mater.*, 2006, **24**, p 399–404
14. G.S. Fox-Rabinovich, B.D. Beake, J.L. Endrino, S.C. Veldhuis, R. Parkinson, L.S. Shuster, and M.S. Migranov, Effect of Mechanical Properties Measured at Room and Elevated Temperatures on the Wear Resistance of Cutting Tools with TiAlN and AlCrN Coatings, *Surf. Coat. Technol.*, 2006, **200**, p 5738–5742
15. M.C. Shaw, *Metal Cutting Principles*, 2nd ed., Oxford University Press, New York, 2005